Hindawi Publishing Corporation
Journal of Nanomaterials
Volume 2013, Article ID 820901, 7 pages
http://dx.doi.org/10.1155/2013/820901

*Research Article*

# Flame Retardancy Effects of Graphene Nanoplatelet/Carbon Nanotube Hybrid Membranes on Carbon Fiber Reinforced Epoxy Composites

**Dongxian Zhuo, Rui Wang, Lixin Wu, Yanhua Guo, Lin Ma, Zixiang Weng, and Jinyu Qi**

*State Key Laboratory of Structural Chemistry, Fujian Institute of Research on the Structure of Matter, Chinese Academy of Sciences, Fuzhou 350002, China*

Correspondence should be addressed to Lixin Wu; lxwu@fjirsm.ac.cn

Received 7 May 2013; Accepted 14 June 2013

Academic Editor: Guohua Chen



Carbon nanotube/graphene nanoplatelet (MWCNT/GNP) hybrid membranes with lower liquid permeability and better barrier effect compared to MWCNT membranes were successfully synthesized by vacuum filtering. Their morphologies, water permeability, and pore structures were characterized by a scanning electron microscope (SEM) and nitrogen adsorption isotherms. Furthermore, MWCNT/GNP membranes were used to improve the flame retardancy of carbon fiber reinforced polymer (CFRP) composites, and the influence of weight percentage of GNPs on the permeability and flame retardancy of MWCNT/GNP membranes was systematically investigated. Results show that incorporation of MWCNT/GNP membranes on CFRP composite plates can remarkably improve the flame retardancy of CFRP composites. Specifically, the incorporation of hierarchical MWCNT/GNP membrane with 7.5 wt% of GNP displays a 35% reduction in the peak heat release rate (PHRR) for a CFRP composite plate with the epoxy as matrix and a 11% reduction in PHRR compared with the incorporation of MWCNT membrane only. A synergistic flame retarding mechanism is suggested to be attributed to these results, which includes controlling the pore size and penetrative network structure.

## 1. Introduction

Carbon fiber reinforced polymer (CFRP) composites have been extensively used in aerospace systems (aircrafts, space vehicles, satellite systems, etc.), automotive parts (bumper beam, hood, radiator support, roof panel, etc.), sporting goods (racing boats, golf shafts and balls, tennis rackets, snow skis, fishing rods, bicycle frames, race cars, etc.), marine applications (passenger ferries, power boats, buoys, offshore pipelines, etc.), and civil engineering structures (CFRP reinforced bridges). However, CFRP composites are generally combustible because their matrix resins contain both hydrogen and carbon atoms. Sometimes it is desirable or required that CFRP composites would have a better flame retardancy [1–3].

Flame retardants, a large group of polymer additives, are playing a major role in improving the flame retardancy of polymer materials. Flame retardants are mainly based on halogen (bromine and chlorine), phosphorus, inorganic, and melamine compounds. Among these flame retardants, only inorganic fillers are normally nontoxic materials; however, conventional fillers are not efficient flame retardants, and the physical properties of polymers are often badly affected by the addition of fillers.

New flame retardant approaches for polymer materials have been developed using nanoadditives [4–6]. To date, many researches focus on nanoclay [7, 8], carbon nanotubes [9, 10], carbon nanofibers [11, 12], graphene [13, 14], nano silica [15, 16], and polyhedral oligomeric silsesquioxanes [17]. Generally, the addition of inorganic nanoadditives to polymer materials results in the following: (i) the ability to promote flame retardancy and thermal stability of a polymer at very low filling levels, (ii) significant improvement to the physical properties of the polymer rather than degradation, (iii) no environmental or toxicity problem, and (iv) no obvious increase in the weight of the polymer materials. Therefore, nanoparticles have a great potential to be one of the most promising flame retardants.

However, there are two major obstacles that must be overcome for the use of inorganic nanoadditives as efficient flame retardants: (i) aggregation of nanoparticles and (ii) dramatic increase of the resin viscosity at high filling levels [18–21]. First, the barrier effect of nanoadditives is believed to be one of flame retarding mechanisms of nanoadditives. Nanoadditive walls make excellent gas barriers which delay the oxidative degradation of resin during a fire accident. Moreover, the larger surface area of nanoadditives can induce a large amount of char which prevents the resin from suffering heat. However, these nano effects will be minimized if nanoadditives aggregate together driven by the strong van der Waals interaction. Second, the flame retardant effect of nanoadditives will not be significant if the loading of nanoadditives is low. However, the viscosity of a polymer resin rapidly increases with the increased loading of nanoadditives, resulting in fabricating problems of composites, especially, when the resin is applied to CFRP composites. Bubbles generated inside the resins with high viscosity are hard to be removed, and the resins are hard to penetrate into carbon fiber fabrics. Besides the viscosity issue, high loading of nanoadditives is prone to aggregate. Consequently, it is often a challenging work to fabricate a nanocomposite with a certain high loading of nanoadditives and well dispersion of nanoadditives. Thus, the use of nanoadditives as flame retardants is limited.

Recently, Wu and his coworker developed novel flame retardancy carbon fiber reinforced polymeric composites using buckypapers [22–24]. Buckypapers are nonwoven carbon nanotube membranes, in which nanotubes are well dispersed and entangled together. Two layers of buckypapers impregnated with epoxy resin were applied to the heat-radiating surfaces of a CFRP composite plate during the cone calorimeter test. It was found that the peak heat release rate of the CFRP composite plate was reduced by more than 60% and the smoke generation was reduced by 50% during combustion [22]. A piece of buckypaper contains many nanosize voids. The flame retarding mechanism of buckypapers on CFRP composites may be promoting the forming of char and stopping the dripping of thermode-composite products. It was reported that montmorillonite, exfoliated to nanoplates in polymer maxtrix, has a different flame retarding mechanism through creating a "tortuous path" to form the gas barrier [25–27]. It would be interesting if these flame retarding mechanisms can be synergistically applied into CFRP composites.

In this paper, carbon nanotubes and graphene nanoplatelets were used to fabricate hybrid membranes. The hybrid membranes were applied on the surface of CFRP composite plates as flame retarding layers. The water permeability and pore structures of hybrid membranes were analyzed. The synergistic effects of carbon nanotubes and graphenes on the flame retardancy of CFRP composites were studied. The effects of the properties (permeability and pore structure) of buckypaper and hybrid membranes on the flame retardancy of CFRP composites were compared, and the flame retarding mechanism of hybrid membranes on CFRP composites was analyzed.

## 2. Experimental

*2.1. Materials.* The raw materials of graphene nanoplatelets (GNP) with 0.5 $\mu$m to 20 $\mu$m in width and 5 nm to 25 nm in thickness were obtained from the Xiamen Knano Graphite Technology Co. The raw materials of multiwalled carbon nanotubes (MWCNT) with 10–30 $\mu$m in length and 20–50 nm in diameter were obtained from the Chengdu Organic Chemicals Co., Chinese Academy of Sciences. Diglycidyl ether of bisphenol A (Epon 128) was purchased from Shanghai Resin Factory Co. The curing agent diethyltoluenediamine (Ethancure 100) was obtained from the Chongshun Chemical. T700 carbon fiber fabrics (Toray Industries, Inc.) were used as reinforcement.

*2.2. Preparation of MWCNT and MWCNT/GNP Membranes.* MWCNTs were dispersed in water at a concentration of 0.7 mg/mL using a high intensity probe sonicator to make a stable suspension of MWCNTs. Subsequently, a MWCNT membrane was prepared by filtering the MWCNT suspension through a nylon filtering membrane with the aid of vacuum. Following filtration, the MWCNT membrane was thoroughly washed with deionized water and acetone to remove the surfactant. Finally, the MWCNT membrane was carefully peeled off from the filter and dried in a vacuum oven. The membrane was marked as "MWCNT".

MWCNTs and GNPs were dispersed in water at a total concentration of 0.7 mg/mL using a high intensity probe sonicator to make a stable suspension of MWCNT and GNP. Subsequently, the hybrid membranes of MWCNTs and GNPs were fabricated using the same procedure to produce MWCNT/GNP membranes. The hybrid membranes were marked as "MWCNT/GNP$n$", where $n$ represents the weight percentage of GNP in hybrid membrane, and $n$ is 2.5, 5, 7.5, 10, 20, and 25, respectively.

*2.3. Water Permeability of MWCNT and MWCNT/GNP Membranes.* The water permeability of the produced MWCNT or MWCNT/GNP membranes was measured to evaluate the barrier effect of GNPs in a MWCNT membrane. The MWCNT or MWCNT/GNP membranes were placed inside a filter and sealed. Deionized water was added on the membrane and flowed through the MWCNT or MWCNT/GNP membranes along the thickness direction. Vacuum was applied to the filter. The water flow rate, thickness of MWCNT or MWCNT/GNP membranes, surface area of MWCNT or MWCNT/GNP membranes, and vacuum pressure were recorded to calculate the $z$-direction permeability of MWCNT or MWCNT/GNP membranes with 70 ~ 90 $\mu$m in thickness and a nanoscale pore structure. The $z$-direction permeability $K_z$ (saturated permeability) was calculated by the following equation derived from Darcy's law:

$$K_z = \frac{Q\eta L}{AP}, \tag{1}$$

where $Q$ is the flow rate; $\eta$ is the viscosity of water; $L$ is the thickness of prepared membranes; $P$ is the vacuum pressure.

*2.4. Preparation of Carbon Fiber Reinforced Epoxy Composites.* Epoxy/T-700 CFRP composite plates with and without MWCNT or MWCNT/GNP membranes skins were fabricated by using hand layup processing followed by vacuum bagging. Consequently, composite plates were cured at 120°C for 2 h and 180°C for another 2 h and then cooled down to the room temperature. The controlled CFRP composite plate was formed with six layers of T-700 carbon fiber fabrics and was marked as "CF/EP". The flame retarding CFRP composite plates were formed with the addition of MWCNT or MWCNT/GNP membrane skin on both sides of a controlled CFRP composite plate: one piece of MWCNT or MWCNT/GNP membrane was placed on the top, and two pieces of corresponding membranes were placed on the bottom of carbon fiber laminates on a mold. The composite sample was marked as "MWCNT/CF/EP" or "MWCNT/GNP*n*/CF/EP", where *n* represents the weight percentage of GNP in hybrid membranes, and *n* is 2.5, 5, 7.5, 10, 15, 20, and 25, respectively. During cone calorimeter test, the bottom side of the composite, with two layers of MWCNT or MWCNT/GNP membranes, was facing up and was closer to the conical radiant electrical heater.

*2.5. Measurements.* A scanning electron microscope (SEM) (JEOL JEM-2010, Japan) was employed to observe the morphologies of samples. The resolution of the secondary electron image is 1.5 nm under 15 kV. All samples should be dried at 50°C for 24 h before the test.

The specific surface (BET) was performed with an automatic surface analyzer (ASAP2020 M, USA). Prior to the characterization of microstructure, all samples were treated at 350°C for 2 h in $N_2$ atmosphere to remove any residual surfactant.

Flammability of the resins was characterized using a cone calorimeter performed in an FTT device (UK) according to ISO 5660 with an incident flux of 35 kW/m$^2$ using a cone shape heater. Typical results from cone calorimeter reported here were the averages of triplicate. The dimensions of the sample were $(100 \pm 0.02) \times (100 \pm 0.02) \times (3 \pm 0.02)$ mm$^3$.

## 3. Results and Discussion

*3.1.Morphologies of MWCNT and MWCNT/GNP Membranes.* The top-left picture in Figure 1 shows a photograph of a MWCNT/GNP membrane. MWCNT/GNP membranes are flexible and are strong enough as a free-standing membrane. The SEM pictures of MWCNT and MWCNT/GNP membranes are also shown in Figure 1. It can be seen that all MWCNT and MWCNT/GNP membranes are a random, dense, and entangled network, which consists of continuous individual MWCNT or mixed MWCN and GNP self-assembled by van der Waals force during filtration. The size and porous structures of MWCNT and MWCNT/GNP membrane are uniform, indicating that MWCNT and GNP were well dispersed in the suspension. Moreover, both MWCNT and MWCNT/GNP membranes have pores with diameters around 100–500 nm, which are much smaller than those in carbon fiber fabrics.

Interestingly, it can be found that the GNPs not only uniformly dispersed in the MWCNT membrane but also aligned along the membrane plane. This can be explained as the following: the flow of water during the filtering process forced the GNPs to lie on the MWCNT/GNP membrane. Some of the voids in MWCNT membrane were covered by GNPs. This MWCNT/GNP hybrid structure would have a better barrier effect than using MWCNTs alone.

The present developed MWCNT membranes for improving flame retardancy of polymer is typically prepared from single one-dimensional carbon nanotubes through vacuum filtration. Although they can endow the nanoparticle with high loading and good dispersion with polymer, the barrier effect need to be further improved. As we have known, compared with one-dimensional nanoparticles, hierarchical nanoparticles preparing by mixing one-dimensional nanoparticles and two-dimensional nanoparticles can guarantee the good dispersion of two-dimensional nanoparticles and high loading on membranes [28, 29] and thus is expected to successfully endow prepared hierarchical MWCNT/GNP membranes with a better barrier effect. In detail, the hierarchical two-dimensional/one-dimensional hybrid nanoparticles have a better barrier effect through creating a "tortuous Path" than one-dimensional nanoparticle.

*3.2. Permeability of MWCNT and MWCNT/GNP Membranes.* Since the geometry structures of the prepared free-standing membranes were changing from one-dimensional structure to hierarchical structure, it is necessary to characterize their permeability property for evaluating the barrier effect of MWCNT and MWCNT/GNP membranes as shields. The permeability of MWCNT and MWCNT/GNP membranes calculated by (1) are depicted in Figure 2. It can be seen that the permeability of MWCNT/GNP membranes is lower than that of MWCNT membrane; while the former is closely related with the content of GNP, there is an optimum content of GNP to get the minimum permeability. The differences in permeability can be directly attributed to changes in the network of nanoparticles.

In fact, the addition of GNP to MWCNT membrane brings two opposite effects on permeability. On the one hand, GNP has a lower permeability than MWCNT due to the "tortuous Path" created by the two-dimensional structure, so the addition of GNP into MWCNT membranes can prolong the effective pervasive path and then improve the barrier effect of resulting hierarchical network. On the other hand, due to the two-dimension structure, GNPs can be not entangled together. Moreover, the incorporation of GNP into MWCNT may decrease the degree of entanglement of nanotubes and therefore increase the distance between entangled points, resulting in larger size pores compared to a MWCNT membrane. This may decrease the permeability of the resultant network. In the case of a MWCNT membrane with a small content of GNP, the first factor is dominant; while in the case of a MWCNT membrane with a large content of GNP, the second factor is dominant. Therefore, there is an optimum content of GNP to get the best permeability.

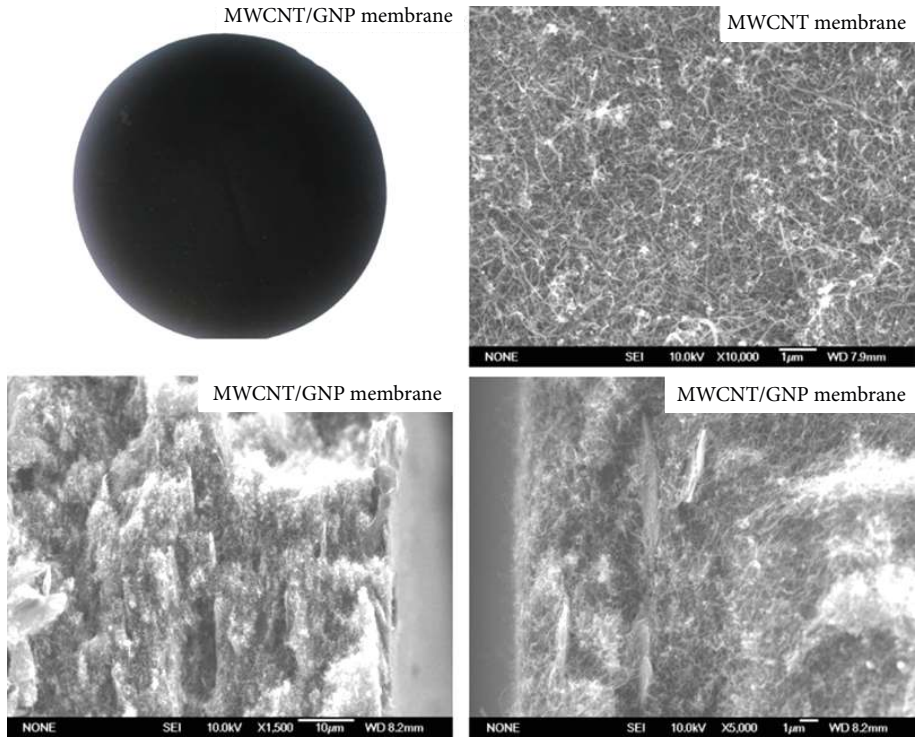


Figure 1: A photograph and SEM pictures of MWCNT and MWCNT/GNP membranes.

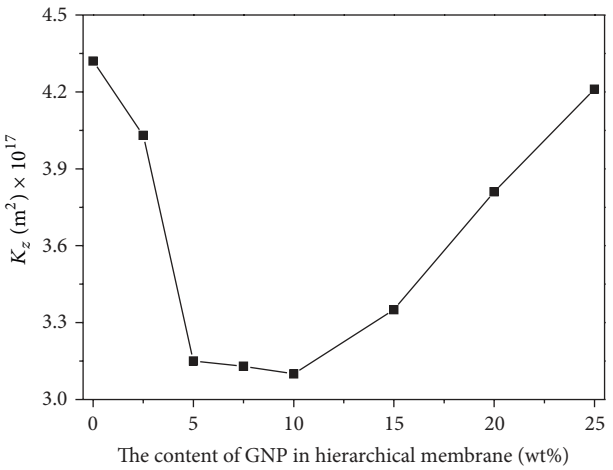


Figure 2: Water permeability of MWCNT and MWCNT/GNP membranes.

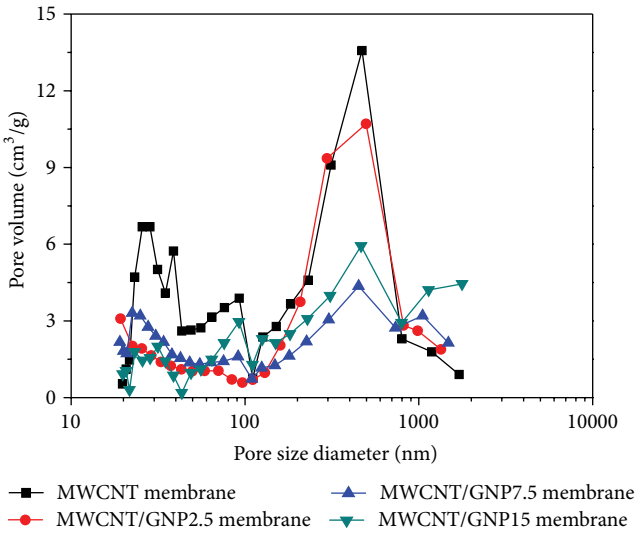


Figure 3: BJH pore analysis of the MWCNT and MWCNT/GNP membranes.

*3.3. Pore Structure and Distribution of MWCNT and MWCNT/GNP Membranes.* The size and distribution of porosity structure for MWCNT and MWCNT/GNP membranes are important characteristics that affect permeability performance. Pore size distributions and BET surface area were determined by nitrogen adsorption isotherms at 77 K, and pore size analysis was performed by BJH method. The pore size distributions of MWCNT and MWCNT/GNP membranes from BJH analysis are shown in Figure 3. Both MWCNT and MWCNT/GNP membranes show a wide macropore peak between 100 nm and 800 nm. For the MWCNT membrane, the peak of macropore size is around 470 nm, and three narrow pore distributions are around 25 nm, 40 nm, and 90 nm. However, as for MWCNT/GNP membranes, the peak of macro-pore size arising from the macroscopic structure of the nanotube or nanoplatelets is still existence about 470 nm, while the previous three narrow pore distributions which relate to the space between nanotube or nanoplatelets aggregates almost disappear, indicating that the incorporating of GNP into MWCNT can

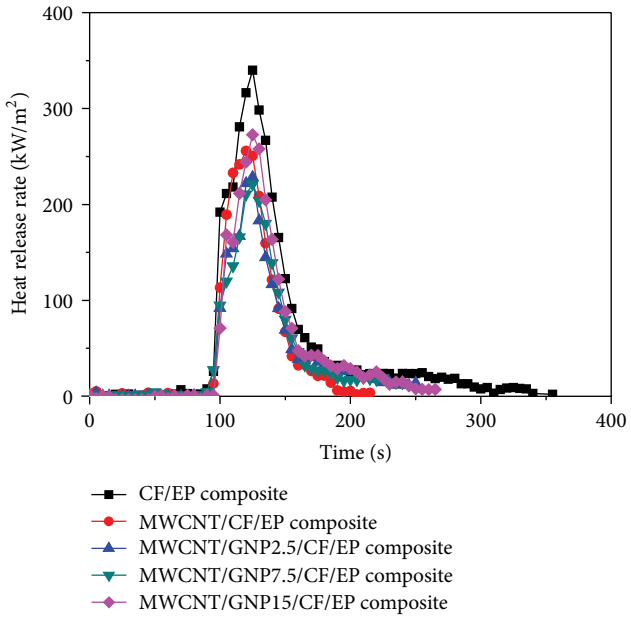


Figure 4: Dependence of heat release rate on time of CF/EP and modified CE/EP composites.

improve the dispersion of MWCNT in resultant network, which is also proven by some investigations [30, 31]. On the other hand, it is interesting to note that the intensities of pore size for MWCNT membranes exceeding 800 nm increase with the continuously increasing content of GNP. This phenomenon can be attributed to the differences in the geometry structure of membranes, which is also agreement with the results of morphology and permeability tests. In addition, the calculated specific surface area ($A_{BET}$) and BJH mean pore width ($d_{BJH}$) are presented in Table 1. The value of $A_{BET}$ for MWCNT membrane is only 86.9 m$^2$ g$^{-1}$ which is less than the previously reported because of its big diameter [22, 32], while the values of $A_{BET}$ for MWCNT/GNP membranes continuously decrease. In summary, MWCNT/GNP membranes show slightly bigger pore sizes than MWCNT membrane, which means that the addition of GNP to MWCNT membrane produces large amounts of pores.

*3.4. Flame Retardancy and Mechanism of MWCNT/CF/EP and MWCNT/GNP/CF/EP Composites.* Generally, the differences in geometry structure and permeability for membranes will undoubtedly affect the flame retardancy of resultant composites. Hence, in order to investigate the detailed flame retardancy, the cone calorimeter was used to evaluate the flame retardancy of modified composite because its results correlate well with those obtained from large-scale fire tests and can be used to predict the combustion behavior of materials in real fires [33]. Figure 4 shows overlay plots of heat release rate (HRR) versus time for CF/EP and modified CE/EP composites; the corresponding data are summarized in Table 2. As for MWCNT/CF/EP composite, the maximum peak (PHRR) displays a 25% reduction with respect to CF/EP composite. However, with regard to MWCNT/GNP/CF/EP

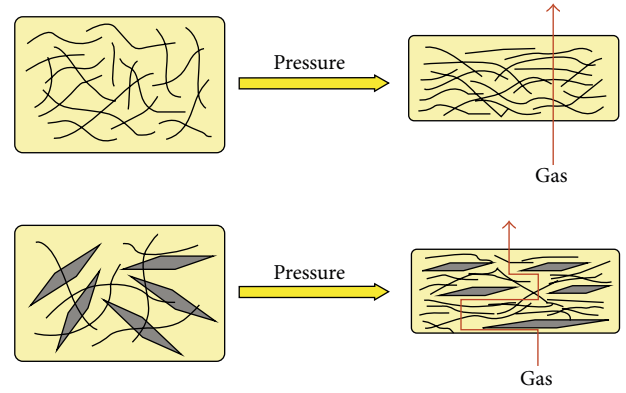


Figure 5: Proposal flame retarding mechanism of hierarchical MWCNT/GNP membranes in carbon fiber reinforced epoxy composite.

Table 1: Porosity of MWCNT and MWCNT/GNP membranes derived from $N_2$ adsorption measurements.

| Sample | $N_2$ isotherms $A_{BET}$ (m$^2$ g$^{-1}$) | Adsorption $d_{BJH}$ (nm, 4 V/A) |
|---|---|---|
| MWCNT membrane | 86.9 | 198 |
| MWCNT/GNP2.5 membrane | 63.8 | 235 |
| MWCNT/GNP7.5 membrane | 50.6 | 262 |
| MWCNT/GNP15 membrane | 51.3 | 369 |

composite, it can be seen that all composites have similar lengths of time for igniting ($t_{ign}$) and time to peak HRR, but the MWCNT/GNP7.5/CF/EP composite displays 35% and 11% reduction in PHRR compared with CF/EP composite and MWCNT/CF/EP composite, respectively; meanwhile, total heat released (THR), total smoke released (TSR), maximum average rate of heat emission (MAHRE) also follow the similar trend, indicating that the MWCNT/GNP membranes can significantly slow down the combustion process and have better flame retardancy effects than MWCNT membranes. However, the flame retardancy seems to deteriorate with the continuously increasing content of GNP in MWCNT membrane. Specifically, the values of PHRR rise from 221.2 kW/m$^2$ for MWCNT/GNP7.5/CF/EP composite to 272.7 kW/m$^2$ for MWCNT/GNP15/CF/EP composite, but the latter is still lower than that of CF/EP composite.

Based on the aforementioned discussions, it can be concluded that a proposal two-mode flame retarding mechanism (Figure 5) is responsible for the greatly improving flame retardancy of CF/EP composite by using hierarchical MWCNT/GNP membranes. In detail, two aspects, the pore size and penetrative network structure, dominate the flame retardancy of the MWCNT/GNP/CF/EP composite. As for MWCNT/CF/EP composites, the general flame retarding mechanism of MWCNT membrane is thought to be the formation of protective barrier during combustion. The macropore diameter of MWCNT membrane determined by nitrogen adsorption isotherms is around 198 nm which is responsible for its high gas permeability, and then the presence of MWCNT membrane on the composite surface

Table 2: Cone calorimeter data for CF/EP and modified CE/EP composites.

| Sample | $T_{ign}$ (s) | PHRR (kW/m$^2$) | THR (MJ/m$^2$) | MAHRE | TSR (m$^2$/m$^2$) | Time to peak HRR (s) |
|---|---|---|---|---|---|---|
| CF/EP | 91 | 339.9 | 17.9 | 82.9 | 707.7 | 125 |
| MWCNT/CF/EP | 93 | 255.8 | 12.7 | 64.3 | 523.4 | 120 |
| MWCNT/GNP2.5/CF/EP | 95 | 228.3 | 11.3 | 56.7 | 438.3 | 125 |
| MWCNT/GNP7.5/CF/EP | 91 | 221.2 | 10.7 | 52.6 | 402.1 | 125 |
| MWCNT/GNP15/CF/EP | 91 | 272.7 | 13.7 | 66.2 | 585.5 | 125 |

can resist decomposed gas release efficiently. Nevertheless, with the incorporating of GNP into MWCNT membrane, their pore sizes tend to increase with the increased content of GNP and then weaken the resistance of gas permeability for MWCNT membrane; at the same time, the introduced two-dimensional structure can exert additional synergistic factor through "Tortuous Path" which can effectively retard the progress of the gas molecules through membranes. These two opposite effects tend to achieve balance, and the flame retardancy reaches its own maximum at an optimum loading of GNP. However, further increasing the content of GNP, the negative factor is dominant and thus has decreased flame retardancy; however this flame retardancy is still greater than that of CF/EP composite owing to the excellent barrier effect of the prepared hierarchical membrane. In a word, through controlling the synergistic effect of the pore size and penetrative network structure, MWCNT/GNP membranes can more effectively reduce the fire hazard of epoxy/T-700 composite by acting as a fire shield than MWCNT membrane, which makes it a promising novel material to improve flame retardancy of polymeric composites.

## 4. Conclusions

Carbon nanotube/graphene nanoplatelet (MWCNT/GNP) hybrid membranes with lower liquid permeability and better barrier effect compared to MWCNT membranes were successfully synthesized by vacuum filtering, which can significantly improve the flame retardancy of carbon fiber reinforced epoxy (CF/EP) composites compared with MWCNT membrane. Specifically, the MWCNT/GNP7.5/CF/EP composite displays 35% and 11% reductions in PHRR compared with CF/EP composite and MWCNT/CF/EP composite, respectively. The improved flame retardancy can be attributed to a flame retarding mechanism including two factors: pore size and penetrative network structure. This investigation issues a new way to develop novel fiber reinforced composites with good flame retardancy.

## Conflict of Interests

The authors declared that they have no conflict of interests.

## Acknowledgments

The authors would like to acknowledge the National Natural Science Foundation of China (Grant no.: U1205114) and Fujian Provincial Key Laboratory of Polymer Materials (Fujian Normal University) for the financial support.

## References

[1] Z. Zhao, J. Gou, S. Bietto, C. Ibeh, and D. Hui, "Fire retardancy of clay/carbon nanofiber hybrid sheet in fiber reinforced polymer composites," *Composites Science and Technology*, vol. 69, no. 13, pp. 2081–2087, 2009.

[2] D. Könnicke, A. Kühn, T. Mahrholz, and M. Sinapius, "Polymer nanocomposites based on epoxy resin and ATH as a new flame retardant for CFRP: preparation and thermal characterisation," *Journal of Materials Science*, vol. 46, no. 21, pp. 7046–7055, 2011.

[3] B. Perret, B. Schartel, K. Stöß et al., "Novel DOPO-based flame retardants in high-performance carbon fibre epoxy composites for aviation," *European Polymer Journal*, vol. 47, no. 5, pp. 1081–1089, 2011.

[4] N. A. Isitman, M. Dogan, E. Bayramli, and C. Kaynak, "The role of nanoparticle geometry in flame retardancy of polylactide nanocomposites containing aluminium phosphinate," *Polymer Degradation and Stability*, vol. 97, no. 8, pp. 1285–1296, 2012.

[5] N. A. Isitman and C. Kaynak, "Nanoclay and carbon nanotubes as potential synergists of an organophosphorus flame-retardant in poly(methyl methacrylate)," *Polymer Degradation and Stability*, vol. 95, no. 9, pp. 1523–1532, 2010.

[6] W. Dong, X. Zhang, Y. Liu et al., "Flame retardant nanocomposites of polyamide 6/clay/silicone rubber with high toughness and good flowability," *Polymer*, vol. 47, no. 19, pp. 6874–6879, 2006.

[7] J. W. Gilman, "Flammability and thermal stability studies of polymer layered-silicate (clay) nanocomposites," *Applied Clay Science*, vol. 15, no. 1-2, pp. 31–49, 1999.

[8] P. Jash and C. A. Wilkie, "Effects of surfactants on the thermal and fire properties of poly(methyl methacrylate)/clay nanocomposites," *Polymer Degradation and Stability*, vol. 88, no. 3, pp. 401–406, 2005.

[9] T. Kashiwagi, F. Du, K. I. Winey et al., "Flammability properties of polymer nanocomposites with single-walled carbon nanotubes: effects of nanotube dispersion and concentration," *Polymer*, vol. 46, no. 2, pp. 471–481, 2005.

[10] T. Kashiwagi, F. Du, J. F. Douglas, K. I. Winey, R. H. Harris Jr., and J. R. Shields, "Nanoparticle networks reduce the flammability of polymer nanocomposites," *Nature Materials*, vol. 4, no. 12, pp. 928–933, 2005.

[11] Y. Tang, J. Zhuge, J. Gou, R. Chen, C. Ibeh, and Y. Hu, "Morphology, thermal stability, and flammability of polymer matrix composites coated with hybrid nanopapers," *Polymers for Advanced Technologies*, vol. 22, no. 10, pp. 1403–1413, 2011.

[12] S. C. Lao, W. Yong, K. Nguyen et al., "Flame-retardant polyamide 11 and 12 nanocomposites: processing, morphology, and

mechanical properties," *Journal of Composite Materials*, vol. 44, pp. 1403–1413, 2010.

[13] P. A. Song, L. N. Liu, S. Y. Fu et al., "Striking multiple synergies created by combining reduced graphene oxides and carbon nanotubes for polymer nanocomposites," *Nanotechnology*, vol. 24, no. 12, pp. 25704–25704, 2013.

[14] S. Liao, P. Liu, M. Hsiao et al., "One-step reduction and functionalization of graphene oxide with phosphorus-based compound to produce flame-retardant epoxy nanocomposite," *Industrial and Engineering Chemistry Research*, vol. 51, no. 12, pp. 4573–4581, 2012.

[15] Y. Chiu, H. Tsai, and T. Imae, "Thermal and morphology properties of various silica contents in sulfone epoxy nanocomposites," *Journal of Applied Polymer Science*, vol. 125, supplement 1, pp. 523–531, 2012.

[16] N. Cinausero, N. Azema, J.-M. Lopez-Cuesta, M. Cochez, and M. Ferriol, "Synergistic effect between hydrophobic oxide nanoparticles and ammonium polyphosphate on fire properties of poly(methyl methacrylate) and polystyrene," *Polymer Degradation and Stability*, vol. 96, no. 8, pp. 1445–1454, 2011.

[17] W. C. Zhang, X. M. Li, Y. Y. Jiang, and R. J. Yang, "Investigations of epoxy resins flame-retarded by phenyl silsesquioxanes of cage and ladder structures," *Polymer Degradation and Stability*, vol. 98, no. 1, pp. 246–254, 2013.

[18] B. K. Deka and T. K. Maji, "Effect of silica nanopowder on the properties of wood flour/polymer composite," *Polymer Engineering and Science*, vol. 52, no. 7, pp. 1516–1523, 2012.

[19] Q. Tai, R. K. K. Yuen, W. Yang, Z. Qiao, L. Song, and Y. Hu, "Iron-montmorillonite and zinc borate as synergistic agents in flame-retardant glass fiber reinforced polyamide 6 composites in combination with melamine polyphosphate," *Composites A*, vol. 43, no. 3, pp. 415–422, 2012.

[20] T. D. Hapuarachchi and T. Peijs, "Multiwalled carbon nanotubes and sepiolite nanoclays as flame retardants for polylactide and its natural fibre reinforced composites," *Composites A*, vol. 41, no. 8, pp. 954–963, 2010.

[21] S. Chapple and R. Anandjiwala, "Flammability of natural fiber-reinforced composites and strategies for fire retardancy: a review," *Journal of Thermoplastic Composite Materials*, vol. 23, no. 6, pp. 871–893, 2010.

[22] Q. Wu, W. Zhu, C. Zhang, Z. Liang, and B. Wang, "Study of fire retardant behavior of carbon nanotube membranes and carbon nanofiber paper in carbon fiber reinforced epoxy composites," *Carbon*, vol. 48, no. 6, pp. 1799–1806, 2010.

[23] Q. Wu, C. Zhang, R. Liang, and B. Wang, "Fire retardancy of a buckypaper membrane," *Carbon*, vol. 46, no. 8, pp. 1159–1174, 2008.

[24] Q. Wu, J. Bao, C. Zhang, R. Liang, and B. Wang, "The effect of thermal stability of carbon nanotubes on the flame retardancy of epoxy and bismaleimide/carbon fiber/buckypaper composites," *Journal of Thermal Analysis and Calorimetry*, vol. 103, no. 1, pp. 237–242, 2011.

[25] S. S. Ray and M. Okamoto, "Polymer/layered silicate nanocomposites: a review from preparation to processing," *Progress in Polymer Science*, vol. 28, no. 11, pp. 1539–1641, 2003.

[26] J. W. Gilman, C. L. Jackson, A. B. Morgan et al., "Flammability properties of polymer—layered-silicate nanocomposites. Polypropylene and polystyrene nanocomposites," *Chemistry of Materials*, vol. 12, no. 7, pp. 1866–1873, 2000.

[27] J. Zhu, A. B. Morgan, F. J. Lamelas, and C. A. Wilkie, "Fire properties of polystyrene-clay nanocomposites," *Chemistry of Materials*, vol. 13, no. 10, pp. 3774–3780, 2001.

[28] U. Khan, I. O'Connor, Y. K. Gun'Ko, and J. N. Coleman, "The preparation of hybrid films of carbon nanotubes and nanographite/graphene with excellent mechanical and electrical properties," *Carbon*, vol. 48, no. 10, pp. 2825–2830, 2010.

[29] M. Yen, M. Hsiao, S. Liao et al., "Preparation of graphene/multi-walled carbon nanotube hybrid and its use as photoanodes of dye-sensitized solar cells," *Carbon*, vol. 49, no. 11, pp. 3597–3606, 2011.

[30] S. Yang, K. Chang, H. Tien et al., "Design and tailoring of a hierarchical graphene-carbon nanotube architecture for supercapacitors," *Journal of Materials Chemistry*, vol. 21, no. 7, pp. 2374–2380, 2011.

[31] A. Yu, P. Ramesh, X. Sun, E. Bekyarova, M. E. Itkis, and R. C. Haddon, "Enhanced thermal conductivity in a hybrid graphite nanoplatelet—carbon nanotube filler for epoxy composites," *Advanced Materials*, vol. 20, no. 24, pp. 4740–4744, 2008.

[32] W. Knapp and D. Schleussner, "Field-emission characteristics of carbon buckypaper," *Journal of Vacuum Science and Technology B*, vol. 2, pp. 557–568, 2003.

[33] D. Zhuo, A. Gu, G. Liang, J. Hu, L. Yuan, and X. Chen, "Flame retardancy materials based on a novel fully end-capped hyperbranched polysiloxane and bismaleimide/diallylbisphenol A resin with simultaneously improved integrated performance," *Journal of Materials Chemistry*, vol. 21, no. 18, pp. 6584–6594, 2011.